Biochimica et Biophysica Acta 1852 (2015) 1520–1530

Contents lists available at ScienceDirect

Biochimica et Biophysica Acta

journal homepage: www.elsevier.com/locate/bbadis

p-SMAD2/3 and DICER promote pre-miR-21 processing during pressure overload-associated myocardial remodeling

Raquel García [a,b], J. Francisco Nistal [b,c], David Merino [a,b], Nathan L. Price [d,e], Carlos Fernández-Hernando [d,e], Javier Beaumont [f], Arantxa González [f], María A. Hurlé [a,b,*], Ana V. Villar [a,b]

[a] Departamento de Fisiología y Farmacología, Facultad de Medicina, Universidad de Cantabria, Santander, Spain
[b] Instituto de Investigación Marqués de Valdecilla (IDIVAL), Santander, Spain
[c] Servicio de Cirugía Cardiovascular, Hospital Universitario Marqués de Valdecilla, Santander, Spain
[d] Vascular Biology and Therapeutics Program, Yale University School of Medicine, New Haven, CT, USA
[e] Integrative Cell Signaling and Neurobiology of Metabolism Program, Section of Comparative Medicine, Yale University School of Medicine, New Haven, CT, USA
[f] Programa de Enfermedades Cardiovasculares, Centro de Investigación Médica Aplicada (CIMA), Universidad de Navarra, Pamplona, Spain

ARTICLE INFO

Article history:
Received 11 December 2014
Received in revised form 23 March 2015
Accepted 7 April 2015
Available online 15 April 2015

Keywords:
Pre-miR-21
p-SMAD2/3
Myocardial fibrosis
Pressure overload
DICER
TGF-β

ABSTRACT

Transforming growth factor-β (TGF-β) induces miR-21 expression which contributes to fibrotic events in the left ventricle (LV) under pressure overload. SMAD effectors of TGF-β signaling interact with DROSHA to promote primary miR-21 processing into precursor miR-21 (pre-miR-21). We hypothesize that p-SMAD-2 and -3 also interact with DICER1 to regulate the processing of pre-miR-21 to mature miR-21 in cardiac fibroblasts under experimental and clinical pressure overload. The subjects of the study were mice undergoing transverse aortic constriction (TAC) and patients with aortic stenosis (AS). In vitro, NIH-3T3 fibroblasts transfected with pre-miR-21 responded to TGF-β1 stimulation by overexpressing miR-21. Overexpression and silencing of SMAD2/3 resulted in higher and lower production of mature miR-21, respectively. DICER1 co-precipitated along with SMAD2/3 and both proteins were up-regulated in the LV from TAC-mice. Pre-miR-21 was isolated bound to the DICER1 maturation complex. Immunofluorescence analysis revealed co-localization of p-SMAD2/3 and DICER1 in NIH-3T3 and mouse cardiac fibroblasts. DICER1-p-SMAD2/3 protein–protein interaction was confirmed by in situ proximity ligation assay. Myocardial up-regulation of DICER1 constituted a response to pressure overload in TAC-mice. DICER mRNA levels correlated directly with those of TGF-β1, SMAD2 and SMAD3. In the LV from AS patients, DICER mRNA was up-regulated and its transcript levels correlated directly with TGF-β1, SMAD2, and SMAD3. Our results support that p-SMAD2/3 interacts with DICER1 to promote pre-miR-21 processing to mature miR-21. This new TGFβ-dependent regulatory mechanism is involved in miR-21 overexpression in cultured fibroblasts, and in the pressure overloaded LV of mice and human patients.

1. Introduction

The left ventricle (LV), when subjected to chronic hemodynamic stress as occurs in valvular aortic stenosis (AS) or hypertension, undergoes a pathological remodeling process, which is characterized by the hypertrophic growth of cardiomyocytes and accumulation of extracellular matrix proteins in the myocardium. The resulting structural changes contribute to the development of contractile dysfunction, which evolves to heart failure [1].

MicroRNAs (miRNAs) are noncoding single-stranded RNAs, approximately 22 nucleotides (nt) in length that are involved in the post-transcriptional control of gene expression [2]. MiRNA genes are usually transcribed by RNA polymerase II, and a single primary transcript of miRNA (pri-miRNA) may contain various miRNA precursors [3]. The biogenesis of specific functional miRNAs requires a two-step maturation process. The RNase DROSHA initiates miRNA maturation in the nucleus by cleavage of the stem loops of pri-miRNAs that are converted into ~70 nt hairpin precursors (pre-miRNAs) [4]. DROSHA forms a macromolecular protein assembly (termed Microprocessor complex) with DiGeorge Syndrome Critical Region 8 (DGCR8) and several cofactors, which are crucial for the accuracy and activity of DROSHA cleavage [4,5]. After transport to the cytoplasm, pre-miRNAs undergo a further processing step mediated by the RNase DICER, which generates a duplex miRNA/miRNA* of 19–25 nt [6]. DICER interacts with different partners

Abbreviations: Ago, Argonaute; AS, aortic stenosis; BAMBI, BMP and activin membrane-bound inhibitor; DGCR8, DiGeorge Syndrome Critical Region 8; LV, left ventricle; miRNA, microRNA; pre-miRNA, microRNA precursor; pri-miRNA, microRNA primary transcript; R-SBE, RNA-SMAD binding element; SPRY1, Sprouty-1; TAC, transverse aortic constriction; TDP-43, transactivation-responsive DNA-binding protein-43; TGF-β, transforming growth factor-β; TRBP, trans-activation response RNA-binding protein

* Corresponding author at: Departamento de Fisiología y Farmacología, Facultad de Medicina, Universidad de Cantabria, E-39011 Santander, Spain. Tel.: +34 942 201 981; fax: +34 942 201 903.
E-mail address: hurlem@unican.es (M.A. Hurlé).

http://dx.doi.org/10.1016/j.bbadis.2015.04.006
0925-4439/

either to complete pre-miRNA cleavage or to recruit Argonaute (Ago) proteins [7,8]. One strand of the mature miRNA together with Ago is loaded into the RNA-induced silencing complex (RISC) and helps in the guidance of RISC to target mRNAs [9]. MiRNAs interact with their cognate mRNAs leading to their translational repression and/or degradation [9].

These small non-coding RNAs have emerged as major regulators of cellular processes involved in the developmental biology, physiology and pathology of the cardiovascular system, with potential clinical applications [10–12]. The harmonious interplay between the miRNAs expressed by the heart is a requirement to keep balanced cardiac morphology, structure and function [13,14]. Specific miRNAs have been implicated in the progression of heart diseases [10] and miR-21 is one of the most consistently up-regulated during cardiac biomechanical stress in experimental models and human pathologies [13–16,21].

Transforming growth factor (TGF-β) plays crucial pathophysiological roles in the maladaptive remodeling of the heart in response to pressure overload by triggering interstitial fibrosis and cardiomyocyte hypertrophic growth [17–19]. Several reports provide evidence that miR-21 acts as a downstream effector of TGF-β signaling to expand pathological fibrosis in different tissues [20,21]. In the myocardium under biomechanical stress, TGF-β induces miR-21 up-regulation, which contributes to maladaptive remodeling both in mice [15] and in AS patients [22]. Davis et al. [23,24] investigated the molecular pathways underlying TGF-β-mediated induction of miR-21 in vascular smooth muscle cells (VSMCs), and showed that the SMAD2/3 canonical effectors of TGF-β signaling promote post-transcriptional cleavage of pri-miR-21 into pre-miR-21 by DROSHA. SMADs bind RNA-SMAD binding element (R-SBE) within the stem region of the primary transcripts of miRNAs regulated by TGF-β, which is similar to the SBE found in the promoters of TGF-β target-genes [23–25]. However, the potential role for TGF-β signaling in the cleavage of pre-miR21 by the ribonuclease III DICER1 remains hitherto unexplored.

Herein, we assess the role of the TGF-β signaling effectors SMAD2/3 in the processing of pre-miR-21 by DICER1 to yield mature miR-21 in fibroblasts. We also explored the functional coupling between activated SMAD2/3 and DICER1 to control the biogenesis of miR-21 during the LV remodeling response to pressure overload in mice subjected to transverse aortic constriction (TAC). The clinical relevance of such interaction was confirmed in LV biopsies from severe AS patients.

2. Methods

2.1. Pressure overload studies in mice

Adult (16–20 weeks old) C57BL6 mice were housed in a room kept at 22 °C with 12:12 h light/dark cycle and provided with standard food and water ad libitum. The study was approved by the University of Cantabria Institutional Laboratory Animal Care and Use Committee and conducted in accordance with the "European Directive for the Protection of Vertebrate Animals Used for Experimental and Other Scientific Purposes" (European Communities Council Directive 86/606/EEC).

LV pressure overload was induced by transverse aortic constriction (TAC). The mice (n = 5 to 12 per group) were anesthetized by intraperitoneal injection of ketamine (10 mg/kg) and xylazine (15 mg/kg) as described [15]. They were subjected to TAC or sham surgery and euthanized 6 h, 12 h or 2 weeks after surgery.

2.2. Pressure overload studies in patients

The study followed the Declaration of Helsinki guidelines for biomedical research involving human subjects. The institutional ethics and clinical research committee approved the study, and all patients gave written informed consent. The clinical and demographic characteristics of the AS and control groups are shown in Supplemental Table S1. The study was performed using LV myocardial intraoperative biopsies obtained from a cohort of 67 consecutive patients diagnosed with isolated severe AS and undergoing aortic valve replacement surgery in the University Hospital Marqués de Valdecilla in Santander, Spain. Patients with aortic or mitral regurgitation greater than mild or with major coronary stenosis greater than 50%, previous cardiac operations, malignancies or poor renal or hepatic function were deemed ineligible for the study. The control group for comparing the myocardial gene expression was a cohort of 30 surgical patients with pathologies (atrial septal defect: n = 18, aortic aneurysm: n = 6, mitral stenosis: n = 3, left atrial myxoma: n = 2, pulmonary valve fibroelastoma: n = 1) that did not include pressure or volume overload, coronary heart disease or cardiomyopathies. Subepicardial biopsies (4 to 10 mg) were taken from the LV lateral wall with a Tru-cut needle during the surgical procedure and snap frozen in liquid nitrogen.

2.3. NIH-3 T3 cell culture

NIH-3 T3 fibroblasts (ATCC, USA) were cultured in Dulbecco's Modified Eagle's Medium (DMEM) supplemented with 10% FBS (Biological Industries, Israel), 100 U/ml penicillin-streptomycin, at 37 °C in 5% CO_2. The cells (2×10^5) were plated in 35 mm culture dish and, 24 h later, they were transiently transfected with pre-miR-21 (1 and 10 nM) or control miRNA (Ambion, Inc) using X-tremeGENE 9 DNA transfection reagent (Roche Diagnostics, Germany). In a series of experiments, the cells were transfected with siSMAD2/3 or scrambled siRNA (Santa Cruz Biotech. Inc), pCIG-ORF-SMAD2 (0.6 μg/ml), pCIG-ORF-SMAD3 (0.6 μg/ml) or empty pCIG vector (1.2 μg/ml; kindly given by Dr. Martí (Parc Cientific, Barcelona, Spain)). In another series of assays, SIS3 (selective inhibitor of SMAD3; Calbiochem), and SB431542 [specific inhibitor of the TGF-β type 1 receptors ALK4, ALK5 and ALK7; (Sigma Aldrich)], were used to block SMAD3 and SMAD2/3, respectively. Four hours later, cells were incubated with recombinant TGF-β1 (0.30 ng/ml) (R&D Systems) for 24 h. The experiments were performed in triplicate and repeated on three separate occasions.

2.4. Luciferase reporter assays

NIH 3T3 cells were seeded in 96 well plates (2×10^4/well) and cultured in the presence of recombinant TGF-β1 (0.3 ng/ml) for 24 h. Cells were co-transfected with a mixture of miR-21 (10 nM), or scrambled miRNA (Ambion, Inc), and pMIR-reporter luciferase vector containing the 3′-UTR of TGF-β1 or SMAD7 in the pMIR-reporter β-Gal (β-galactosidase) vector (50 ng), using X-tremeGENE 9 DNA transfection reagent (Roche Diagnostics, Germany). Luciferase activity was assessed after 24 h using a Luciferase® Reporter Assay System (Promega) according to the manufacturer's specifications. Transfection and luciferase assays were performed in triplicate and repeated on three separate occasions.

2.5. Primary culture of mouse cardiac fibroblasts

Adult cardiac fibroblasts were isolated from 4 month-old C57BL6 mice by enzymatic digestion as previously described [15]. For experimental procedures, low passage cells (p2) were seeded onto 35 mm cell culture dishes and incubated at 37 °C, in 5% CO_2, for 15–20 h. The cells were growth arrested by incubation in DMEM containing 10% FBS and 10% DBS for 12 h.

2.6. MiR-21 detection by in situ hybridization

MiR-21 in situ hybridization was conducted in NIH-3T3 cells and primary cardiac fibroblasts using miCURY LNA miRNA ISH Kit (Exiqon A/S, Vedbaek, Denmark), which contains a digoxigenin (DIG)-double-labeled specific miR-21 probe (5′-DIG/TCA ACA TCA GTC TGA TAA GCT A/DIG-3′), and a scrambled miRNA probe (5′-DIG/GTG TAA CAC GTC TAT ACG CCC A/DIG-3′) to be used as negative control.

2.7. Immunofluorescence

Fixed NIH-3 T3 cells, primary cardiac fibroblasts and LV sections from TAC mice were incubated overnight with primary antibodies against p-SMAD2/3 (Santa Cruz) and DICER1 (Abcam). Secondary antibodies were conjugated with FITC (Jackson, USA) or Cy3 (Abcam). DAPI (Sigma) was used as a nuclear counterstain. Confocal microscopy was performed with an LSM-510 laser scanning microscope (Carl Zeiss Inc., Germany) using a 40× objective.

2.8. In situ proximity ligation assay

We utilized the Duolink kit for in situ proximity ligation assay (Duolink II, Sigma), following the manufacturer's instructions on NIH-3 T3 cells treated with TGFβ1 (0.3 ng/ml) for 24 h, fixed in paraformaldehyde (4%) and permeabilized with 0.25% Triton-X.

Primary antibodies utilized: rabbit polyclonal anti DICER1 (Abcam), goat polyclonal anti p-SMAD2/3 (Santa Cruz), goat polyclonal anti p-SMAD2 (Santa Cruz), rabbit polyclonal anti p-SMAD3 (Abcam), goat polyclonal anti TGF-β (Santa Cruz) and rabbit polyclonal anti Elk1 (Santa Cruz). Secondary antibodies bear a short DNA strand that hybridizes with an additional circle-forming oligodeoxynucleotide [26,27]. The DNA is then visualized using a fluorescent probe using a Nikon A1R microscope, with a plan apochromatic 60 × 1.4 NA objective operated by the Nis elements software.

2.9. Determination of mRNA and miRNA expressions by q-PCR

Total RNA from the LV myocardium and cultured cells was obtained by TRIzol extraction (Invitrogen). MiRNAs were isolated using a miRNA isolation kit (Nucleo spin miRNA kit, Macherey-Nagel, Germany). The mRNA was reverse transcribed using random primers and the miRNAs were reversed transcribed using specific primers for pre-miR-21, miR-21, cel-miR-39 and RNU6-b (Applied Biosystems). The quantitative PCR (Q-PCR) was performed with specific TaqMan primers: DICER1, TGF-β1, SMAD2, SMAD3, TIMP3, TGF-βR2, miR-21 and SYBR Green primers for pre-miR-21: reverse, 5′-TGTCAGACAGCCCATCGACT-3′ forward, 5′-TGTCGGGTAGCTTATCAGAC-3′ (Sigma-Aldrich). The housekeeping genes were cel-miR-39, 18S and RNU6b. Duplicate transcript levels were determined in a minimum of three independent experiments.

To avoid the confounding influence of factors such as anesthesia, surgery, inflammation, etc., in the group of mice subjected to 6–12 h TAC, mRNA and miRNA relative expressions (vs 18S and RNU6B, respectively) were expressed as fold change in TAC mice versus the average expression of sham operated mice.

2.10. MicroRNA-21 Northern blot analysis

Total RNA (5 μg) was resolved in a 15% polyacrylamide gel and blotted onto a Hybond-N+ nylon membrane (Amersham Biosciences). miRCURY LNA™ microRNA detection probe for hsa-miR-21 was purchased from Exiqon. The oligonucleotide sequence (5′-TCAACATCAG TCTGATAAGCTA-3′), which is complementary to mature miR-21, was end labeled with [α-32P]ATP and T4 polynucleotide kinase (New England BioLabs) to generate highly-specific-activity probes. The oligonucleotide sequence for 5S rRNA was 5′-CAGGCCCGACCCTGCTTAGCTT CCGAGATCAGACGAGAT-3′. Hybridization was carried out according to Express Hyb (Bio-Rad) protocols.

2.11. RNA-immunoprecipitation assays

Polyclonal SMAD2/3 antibody was incubated with Dynabeads protein G (Dynal Biotech, invitrogen), following the manufacturer's protocol. Controls were performed using non-specific IgG-Dynabeads. LV samples were homogenized and lysed in buffer (Tris 50 mM, EDTA 1 mM, SDS 2%) containing a protease inhibitor cocktail (Sigma-Aldrich, pH 7.5). Lysates were incubated with SMAD2/3 Ab-Dynabeads and the eluent was processed for Western blot analysis and for RNA purification using TRIzol reagent. Twenty-five fentomoles of *Caenorhabditis elegans* oligonucleotide (cel-miR-39) were added as a spike-in control [28]. Pre-miR-21 and miR-21 expression levels were determined by q-PCR and normalized to cel-miR-39.

2.12. Protein detection by Western Blot

Samples were resolved on 10% sodium dodecyl sulfate-polyacrylamide (SDS-PAGE) gel and transferred onto polyvinylidene difluoride (PVDF) membranes (Bio-Rad Lab., California, USA). The primary antibodies used were: monoclonal anti DICER (Abcam); polyclonal anti p-SMAD2/3 (Santa Cruz); polyclonal anti GAPDH (Santa Cruz); and polyclonal anti ELK-1 (Santa Cruz). ECL Advance Western Blotting Detection Kit (GE Healthcare Europe GmbH, Munich, Germany) was used for immunodetection.

2.13. Statistics

The data sets were assessed for normality with the Kolmogorov–Smirnov test. Continuous variables were compared using two-tailed Student's *t*-test or Mann–Whitney *U* test. Correlations between the expression levels of miR-21 and cardiac remodeling genes were performed using Pearson's correlation analysis. Statistical packages: GraphPad Prism 5.03 and PASW Statistics 18 (SPSS Inc., Chicago, IL).

3. Results

3.1. p-SMAD2/3 proteins participate in the maturation of pre-miR-21 to miR-21 upon TGF-β1 stimulation

The SMAD effectors of TGF-β signaling control the transcription of pri-miR-21 and its subsequent post-transcriptional nuclear conversion into pre-miR-21 [23,29]. Herein, we assessed whether p-SMAD2/3 regulates also the last step of miR-21 maturation, i.e. the processing of pre-miR-21 to mature miR-21. For this purpose, NIH-3 T3 fibroblasts were transfected with pre-miR-21, SMAD2/3 and siSMAD2/3 and the expression levels of pre-miR-21 and miR-21 were detected by Northern blot (Fig. 1A). Concomitant transfection of the cells with pre-miR-21 (10 nM) and pCIG-ORF-SMAD2 (0.6 μg/ml) and pCIG-ORF-SMAD3 (0.6 μg/ml) increased the production of mature miR-21 (1.7 ± 0.2 fold vs control, $p < 0.01$; Fig. 1A lane 3, and densitogram in Fig. 1C), while the expression of its precursor was reduced (0.6 ± 0.2 fold vs control, $p < 0.05$; Fig. 1A lane 3, and densitogram in Fig. 1B). Silencing SMADs with siRNAs (10 nM) prevented the overproduction of mature miR-21 induced by pCIG-ORF-SMAD2 and pCIG-ORF-SMAD3 (0.9 ± 0.1 fold vs control; Fig. 1A lane 4, and densitogram in Fig. 1C) and consequently, pre-miR-21 expression increased (2.1 ± 0.2 fold vs. control, $p < 0.001$; Fig. 1A lane 4, and densitogram in Fig. 1B). Western blot experiments confirmed the reduction of SMAD2/3 protein expression in cells treated with siSMAD2/3 (Fig. 1F and densitograms in Fig. 1H and I), which resulted in miR-21 down-regulation and pre-miR-21 accumulation as determined by qPCR (Fig. 1D and D′). The expression of DICER1 protein was not altered after silencing SMAD2/3; therefore, the impaired processing of miR-21 by the cells was not due to reduced expression of DICER1 (Fig. 1F and densitogram in Fig. 1G). Chemical inhibition of SMAD2 and SMAD3 with SB431542 confirmed the reduction of miR-21 production and the accumulation of pre-miR-21 observed after knocking-down SMAD2/3 using siRNAs (Fig. 1 E and E′). Of note, the selective inhibition of SMAD3 with SIS3 produced a similar degree of miR-21 down-regulation to the inhibition of both SMADs with SB431542. These results, although they do not exclude a role for SMAD2, suggest a preeminent contribution of SMAD3 to the TGF-β-dependent regulation of DICER1 endonuclease activity.

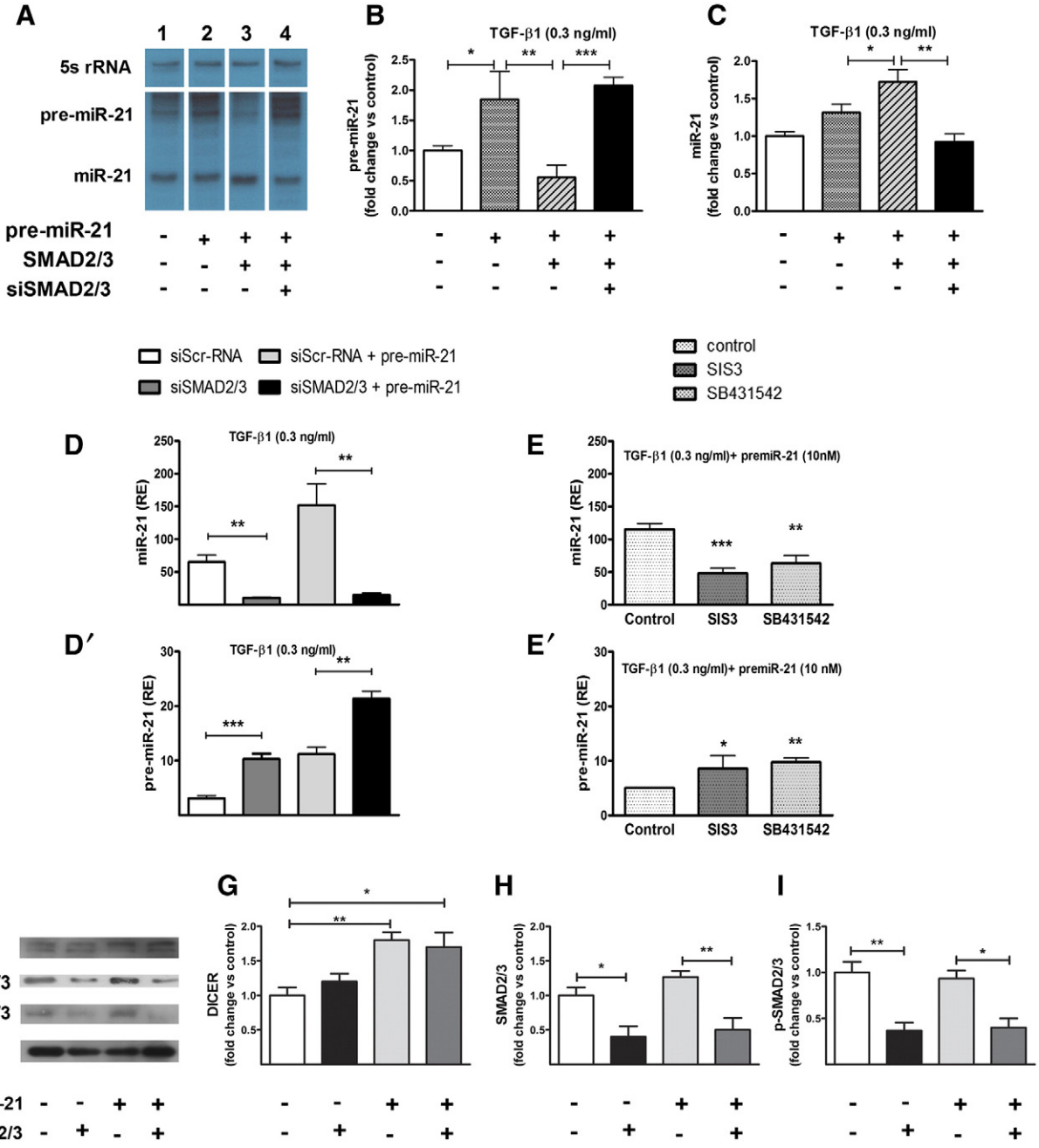

Fig. 1. A: Representative Northern blot showing the expression levels of pre-miR-21 and miR-21 in NIH-3 T3 cells cultured in the presence of TGF-β1. Cells were non-transfected (lane 1) or transfected with pre-miR-21 (lanes 2, 3 and 4), SMAD2 + SMAD3 (lanes 3 and 4) and siSMAD2/3 (lane 4). 5S rRNA was used as a loading control. The blots belong to the same gel. B and C: Densitograms of pre-miR-21 (B) and miR-21 (C) expression as relative fold change vs. non transfected cells (open column of the histograms). D and E: Effects of recombinant TGF-β1 on mature miR-21 (D and E) and pre-miR-21 (D′ and E′) expression levels, determined in the same cells. Knocking-down SMAD2/3 with siSMAD2/3 or chemical inhibition with SB431542 resulted in lower production of mature miR-21 and accumulation of pre-miR-21. Similar effects were observed with the selective chemical inhibitor of SMAD3, SIS3. F: Representative Western blots showing the protein levels of DICER1, SMAD2/3 and p-SMAD2/3 in NIH-3 T3 cells transfected with pre-miR-21 or scrambled oligonucleotides and siSmad2/3 or scrambled siRNA. GAPDH was used as loading control. G, H and I: Densitograms of DICER1 (G), SMAD2/3 (H) and p-SMAD2/3 (I) protein expression as relative fold change vs. control cells (first dot of each Western blot) (*$p < 0.05$, **$p < 0.01$, ***$p < 0.001$, ANOVA followed by Bonferroni).

The capability of TGF-β1 to activate its canonical signaling pathway in this particular cell line was already reported [22]. After cell activation with TGF-β1 (0.3 ng/ml), the maximal overexpression of SMAD2/3 and its active form p-SMAD2/3 was observed at 24 h (supplementary Fig S1). Moreover, an increment in pre-miR-21 levels resulted in a significant increase in mature miR-21 (supplementary Fig S2). Overall, our in vitro results support the involvement of active SMAD2/3 (phosphorylated form) in the processing of pre-miR-21 to mature miR-21 by DICER1 in NIH-3 T3 fibroblasts (a schematic representation of this process is depicted in Fig. 7).

3.2. p-SMAD2/3 physically interacts with DICER1 within NIH-3 T3 cells

To determine whether p-SMAD2/3 and DICER1 co-localize in similar cellular compartments we performed confocal immunofluorescence analysis in NIH-3 T3 fibroblasts treated with recombinant TGF-β1. The results revealed a marked co-localization of p-SMAD2/3 and DICER1 fluorescence signals in the perinuclear region, suggesting that DICER1 and p-SMAD2/3 might interact in the same functional complex (Fig. 2A). We further assessed whether p-SMAD2/3 interacts directly and specifically with DICER1 using in situ proximity ligation assay

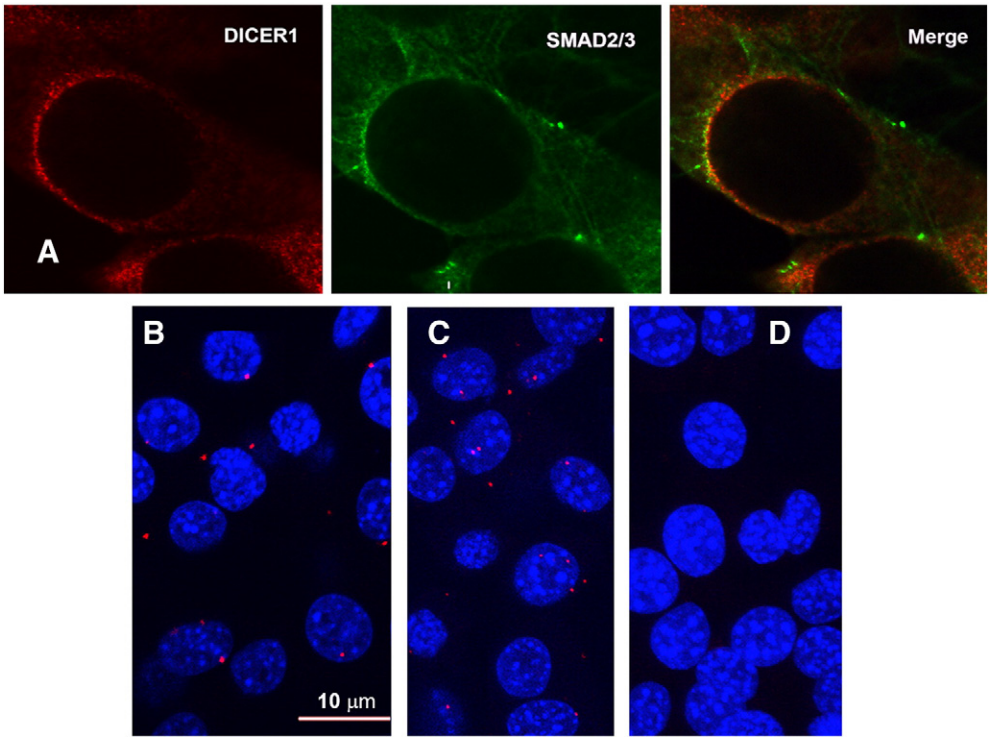

Fig. 2. DICER1 and p-SMAD2/3 co-localize in NIH-3T3 fibroblasts. A: Representative confocal immunofluorescence images showing DICER1 (red) and p-SMAD2/3 (green) in NIH-3 T3 cells. The merged panel shows DICER1/p-SMAD2/3 co-localization (yellow). B, C and D: In situ protein–protein association between DICER1 and p-SMAD2/3 detected by proximity ligation assay (PLA). B: Proximity ligation signals (red) in NIH-3 T3 cells using rabbit polyclonal anti-DICER1 and goat polyclonal anti-p-SMAD2/3 antibodies. Nuclei were counterstained with DAPI (blue). Each red dot represents a protein–protein association complex. C: Positive control experiment using goat polyclonal anti-p-SMAD3 and rabbit polyclonal anti-p-SMAD2 antibodies. D: Negative control experiment using primary antibodies directed against non-interacting proteins such as ELK-1 and TGF-β.

(PLA). Two primary antibodies were used, one targeting each of the investigated proteins in an expected interaction (i.e. DICER1 and p-SMAD2/3). As shown in Fig. 2B, in situ proximity ligation assay gave a bright signal within the spots where DICER1 and p-SMAD2/3 presented a physical interaction. The perinuclear localization of the PLA fluorescence is in agreement with the confocal immunofluorescence observations. Taken together, our results demonstrate the capability of p-SMAD2/3 to physically interact with DICER1 to form protein-protein complexes in NIH-3T3 cells (a schematic representation is shown in Fig. 7). The positive control showed p-SMAD2/p-SMAD3 complexes scattered in both the nucleus and cytoplasm of the cells. No positive signal was detected using primary antibodies directed against non-interacting proteins such as ELK-1 and TGF-β as a negative control.

3.3. miR-21 targets 3′UTR of SMAD7 but not 3′UTR of TGF-β1 in NIH-3 T3 cells

Our findings along with previously published work [23–25] indicate that the miR-21 maturation process is tightly regulated by canonical p-SMAD2/3. In turn, several elements of TGF-β pathways are targeted by miR-21 [19,29]. To assess whether TGF-β1 can establish a negative auto-regulatory feed-back loop mediated by miR-21 in fibroblasts, we determined the capability of miR-21 to target the transcripts of TGF-β1. For this purpose, the interaction of miR-21 with the 3′-untranslated region (3′UTR) of TGF-β1 was determined using a luciferase assay in NIH-3 T3 cells. As a positive control, cells were transfected with the 3′ UTR of SMAD7, an inhibitory element of the TGF-β signaling, which

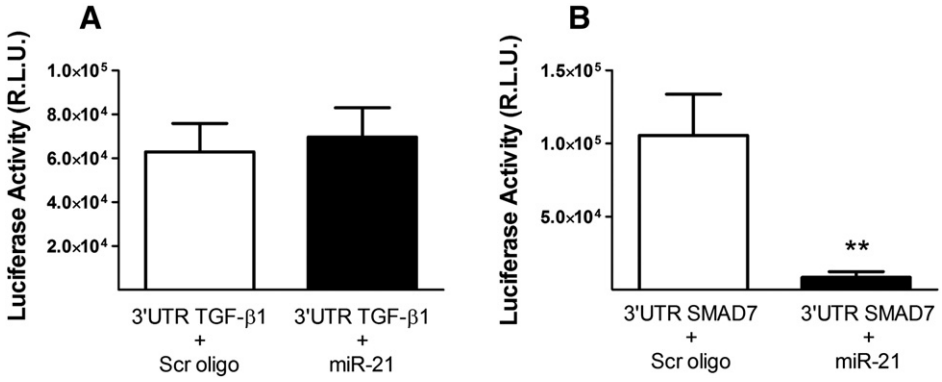

Fig. 3. SMAD7, but not TGF-β1, is targeted by miR-21. A and B: Luciferase activity of the 3′-untranslated region (3′UTR) of human TGF-β1 (A) and the 3′UTR of human SMAD7 (B) in NIH-3 T3 cells co-transfected with miR-21 mimics or with scrambled oligonucleotides (scr-oligos) as negative control. The luciferase assay shows that miR-21 does not reduce luciferase activity in cells transfected with TGF-β1 3′UTR while in the positive control miR-21 markedly reduces luciferase activity in cells transfected with SMAD7 3′UTR (**$p < 0.01$, Student's *t* test).

has been previously reported to be a target of miR-21 in other cell types [19] but not yet in fibroblasts. The luciferase assays (n = 4 independent assays) showed that transfection of miR-21 only reduced the luciferase activity in cells transfected with the 3′UTR of SMAD7, but not in cells overexpressing the 3′UTR of TGF-β1 (Fig. 3).

3.4. Myocardial up-regulation of DICER1 constitutes a LV remodeling response to pressure overload in mice which is directly related to the expression levels of TGF-β1 and its canonical effectors

Next, we hypothesized that TGF-β1 and DICER1 may function together to control miR-21 maturation during the LV remodeling response to pressure overload in mice subjected to TAC. The echocardiographic morphofunctional changes induced by 2 weeks of TAC in mice are depicted in Supplementary Fig. S3.

Our previous [22] and present results (Supplementary Table S2) showed increased expression levels of miR-21 in the pressure overloaded myocardium from TAC mice both in the early (6 and 12 h-TAC) and late (2-week-TAC) phases following aortic constriction, in comparison with the corresponding sham group of mice. In parallel, the transcript levels of TGF-β1 and its canonical effectors (SMAD2 and/or SMAD3) increased significantly after TAC (Supplementary Table S2). The relevance of miR-21 overexpression in the remodeling response to pressure overload was supported by the significant and direct correlation between miR-21 levels and the LV mass ($R = 0.65$, $p < 0.001$) and with the expression levels of extracellular matrix elements such as Col I (0.55, $p < 0.01$) and FN1 (0.69, $p < 0.001$) observed in 2-week-TAC mice (Supplementary Table S3).

The myocardial levels of DICER1 mRNA were significantly up-regulated in TAC mice (Fig. 4 A and A′). DICER1 overexpression correlated significantly and positively with the expression levels of genes encoding TGF-β1 and its canonical effectors SMAD2 and SMAD3 both in the early (6–12 h) and late (2 weeks) TAC mice (Fig. 4B–E). Of note, the relationship between the early DICER1 expression and the rise in TGF-β signaling triggered by pressure overload was further supported by the results of multiple regression analysis. In the resulting model, the transcript levels of TGF-β1, SMAD2 and SMAD3 constituted independent predictors of myocardial DICER1 expression. The regression equation was the following:

$$\mathrm{DICER1} = -1.25 + 0.55[\mathrm{SMAD2}] + 0.31[\mathrm{SMAD3}] + 0.19[\mathrm{TGF}-\beta 1].$$

The adjusted coefficient of determination R^2 (0.70; $p < 0.001$) indicated that 70% of the variance in DICER1 mRNA levels during the first 6–12 h after TAC could be estimated from this model [29]. Additionally, in agreement with our hypothesis, the transcript levels of DICER1 and pre-miR-21 were directly correlated (Fig. 4F, $r = 0.56$; $p < 0.05$).

3.5. The LV myocardium from aortic stenosis patients exhibits overexpression of DICER1 mRNA that is directly related to the expression of TGF-β1 and its canonical effectors

In order to establish the clinical relevance of the results obtained in the pressure overload murine model and their translational potential, we analyzed the relationship between DICER1 mRNA expression and TGF-β signaling in LV biopsies obtained from a cohort of 64 severe AS patients (Supplementary Table S1). As observed in TAC mice, the LV myocardium from AS patients, compared with surgical controls, exhibited increased expression levels of miR-21 and pre-miR-21, DICER 1 and TGF-β1 (Supplementary Table S2 and Fig. 5A). Moreover, similar to our findings in mice, DICER1 mRNA maintained significant positive correlations (Fig. 5B–E) with the expression of genes encoding TGF-β1 ($r = 0.47$; $p < 0.001$), SMAD2 ($r = 0.48$; $p < 0.001$) and SMAD3 ($r = 0.54$; $p < 0.001$), as well as with pre-miR-21 ($r = 0.34$; $p < 0.01$).

3.6. SMAD2/3 and DICER1 interact in the protein complex that regulates the processing of pre-miR-21 in pressure-overloaded mice heart

The co-localization of p-SMAD2/3 and DICER1 that was observed in NIH-3T3 fibroblasts was also assessed in primary fibroblasts from adult C57BL6 mouse hearts incubated in the presence of TGF-β1 and in LV sections from TAC mice. Mature miR-21 was expressed when primary LV fibroblasts were cultured in the presence of recombinant TGF-β1 (0.3 ng/ml), as evidenced by in situ hybridization (Fig. 6A). We also confirmed by confocal immunofluorescence the co-localization of p-SMAD2/3 and DICER1 in the perinuclear region of LV fibroblast in culture (Fig. 6B) and in LV sections from TAC mice (Fig. 6C). Therefore, we postulated that, under biomechanical stress, activated SMAD2/3 and DICER1 could interact within the protein complex that regulates the processing of pre-miR-21. To assess this hypothesis, we performed co-immunoprecipitation–RT-qPCR studies in LV myocardial lysates from mice subjected to TAC pressure overload or sham operated, using an antibody that targets SMAD2/3. We found that DICER1 co-precipitated along with SMAD2/3, and both proteins were significantly up-regulated in the lysates from TAC-mice compared to sham-mice (Fig. 6D–G). RNA bound to the protein complexes was isolated, and a significant increase of pre-miR-21 in TAC vs. sham mice (Fig. 6H) was observed. When anti-SMAD2/3 antibody was substituted by a non-specific IgG in control assays, pre-miR-21 was absent of the immunoprecipitated complexes (data not shown). Densitometry showed a 2.1 fold increase of DICER1 (Fig. 6E sham IP 2.6 ± 0.4 AU vs TAC IP 4.2 ± 0.4 AU, $p < 0.01$ Student's *t* test) and a 1.6 fold increase of SMAD2/3 (Fig. 6F sham IP 1.7 ± 0.1 AU vs TAC IP 2.4 ± 0.3 AU, $^{*}p < 0.05$, $^{**}p < 0.01$ Student's *t* test) expression compared to sham mice. Densitometry of the input is shown in Fig. 6G.

4. Discussion

In the present study, we provide evidence supporting a previously uncharacterized role for the canonical TGF-β signaling pathway in the posttranscriptional processing of pre-miR-21 into mature miR-21, through the interaction of p-SMAD2/3 effectors with the DICER1 processor machinery in fibroblasts. The pathophysiological relevance of this regulatory mechanism in the maladaptive remodeling response of the LV myocardium to pressure overload is supported by our findings in experimental mouse TAC models and in the clinical scenario of aortic valve stenosis.

The control of miRNA biogenesis by TGF-β signaling pathways is an integral step of numerous cellular biological systems under physiological and pathological conditions [29]. TGF-β induces miR-21 overexpression, which contributes to myocardial profibrotic events in murine models [15] and in patients [22]. The canonical effectors of TGF-β signaling control the nuclear steps of miR-21 biogenesis. p-SMAD2 and p-SMAD3 promote transcriptional activation of pri-miR-21 [29] and regulate the subsequent post-transcriptional conversion of pri-miR-21 into pre-miR-21 by DROSHA [25,29]. Herein, we show that NIH-3T3 fibroblasts responded to TGF-β1 stimulation leading to mature miR-21 up-regulation. With the purpose of dissecting the regulatory role of TGF-β signaling on the last step of miR-21 maturation (from pre-miR-21 to miR-21) by the RNase DICER1, NIH-3 T3 fibroblasts were lipid-transfected with the substrate of this reaction, i.e. pre-miR-21. Under these experimental conditions, the cells exhibited an increased production of mature miR-21 at a rate that was dependent on the amount of pre-miR-21 transfected. Moreover, overexpression of pre-miR-21 and SMAD2/3 resulted in an increased expression of miR-21, which was accompanied by a reduction of the precursor. Conversely, down-regulation of SMAD2/3 proteins was associated with a significantly lower production of mature miR-21 and an accumulation of pre-miR-21 within the cells. Such phenomena occurred without any variation in DICER1 expression after SMAD2/3 deregulation. Overall, our results indicate a relevant regulatory role for SMAD2/3 in the maturing process

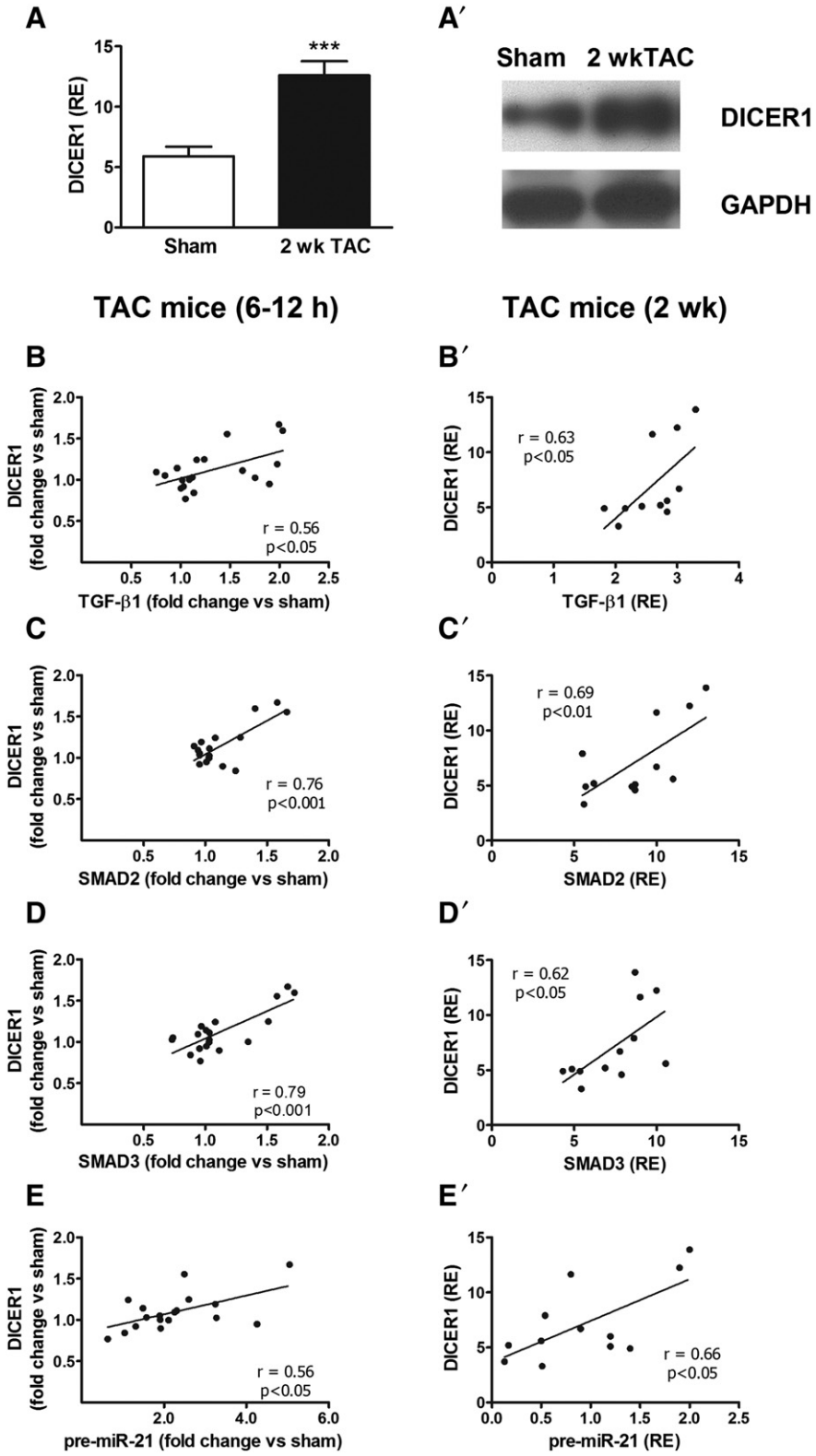

Fig. 4. Pressure overload induces DICER1 up-regulation in the LV of mice subjected to transverse aortic constriction (TAC). A: DICER1 gene relative expression (RE, normalized to 18S) in the LV myocardium from 2 week-TAC and sham operated mice (***$p < 0.001$ vs. sham, Mann–Whitney test). A′: Representative Western blots showing DICER1 protein up-regulation in the LV from 2 week-TAC mice. B to E: Linear regression and Pearson's correlation analyses showing the positive correlation between myocardial DICER1 mRNA and TGF-β1 (B), SMAD2 (C), SMAD3 (D), and pre-miR-21 expression (E) in TAC mice. B to E: In the group of early TAC (6 h and 12 h), gene expression is presented as fold change in TAC mice versus the mean expression of their corresponding group of sham mice. B′ to E′: In the group of 2-week-TAC, gene expression is presented as relative expression (RE) versus 18S ribosomal RNA. r = Pearson's correlation coefficient.

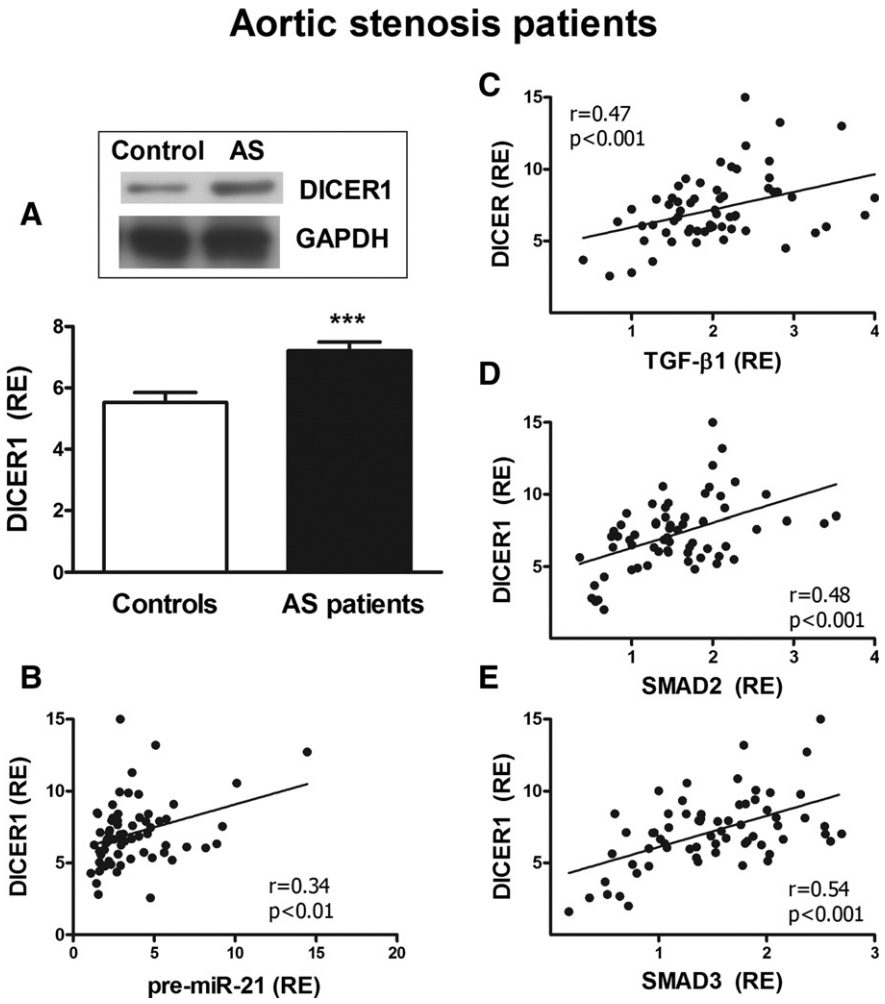

Fig. 5. Pressure overload induces LV up-regulation of DICER1 in aortic stenosis patients. A: DICER1 mRNA expression (RE) normalized to 18S (***$p < 0.001$ vs surgical controls, Mann–Whitney test). Inset: Representative Western blots showing DICER1 expression. B to D: Linear regression and Pearson's correlation analyses showing the positive correlation between myocardial DICER1 and TGF-β1 mRNA expression (B), SMAD2 (C) and SMAD3 (D). r = Pearson's correlation coefficient.

of pre-miR-21 by DICER1 in NIH-3 T3 cells. Whether the interaction between SMAD2/3 and DICER1 could regulate also the maturation of other miRs deserves further investigation.

The perinuclear co-localization of DICER1 and p-SMAD2/3-immunofluorescence signals in NIH-3 T3 cells, in primary cardiac fibroblasts and in LV sections from TAC mice further suggests that both proteins may be part of the same functional complex. In situ proximity ligation assays confirm the existence of a direct protein–protein interaction between p-SMAD2/3 and DICER1 in NIH-3 T3 cells. In situ proximity ligation assays unveil the existence and localization of interactions between two endogenous proteins within the cells [26,27]. Herein, proximity ligation assays and inmunofluorescence approaches detected p-SMAD2/3/DICER1 aggregates in the cytosolic perinuclear region of fibroblasts. This topography is in agreement with the recently proposed idea that the central steps of RNA silencing by miRNAs, including the processing of pre-miRNA to mature miRNAs by DICER1, occur at the cytosolic surface of the rough endoplasmatic reticulum membrane [30-31]. The accurate production of specific functional miRNAs requires protein–protein and protein–RNA interactions mediated by many accessory factors that form complexes with either DROSHA and/or DICER1 [32–35]. The mechanisms that regulate miRNA abundance constitute a subject of active research. The biogenesis of miRNAs is regulated in a complex manner in response to physiological and pathological stimuli. Mechanisms of transcriptional control are relatively well-known [34], but modulation of post-transcriptional processing of miRNA precursors is poorly understood despite evidence that numerous miRNAs are regulated at the posttranscriptional stage [35]. Transient protein complexes, assembled after signal reception, allow for integration of signaling events from many pathways, leading to contextual changes in miRNA expression with the required critical specificity [35,36]. The first study reporting posttranscriptional regulation of miRNA biogenesis by signal transducers demonstrated that members of the TGF-β superfamily of cytokines specifically promote processing of pri-miR-21 in vascular smooth muscle cells [23]. TGF-β and BMP signaling induces a rapid increase in mature miR-21 expression by promoting the processing of pri-miR-21 into pre-miR-21 by the DROSHA microprocessor complex. The sequence-specific association of SMADs to the RNA-SMAD binding elements (R-SBE) within pri-miR-21 provides a platform for microprocessor complex docking and mediates more efficient cleavage by DROSHA [23–25]. Our present results indicate that p-SMAD2/3 can also act as accessory factor of DICER1 and suggest that this direct interaction facilitates the processing of pre-miR-21 into mature miR-21 (schematic representation in Fig. 7). The location of the R-SBE in the middle segment of the mature miR-21 sequence [24,25] suggests that p-SMAD2/3 might serve as an accompanying cofactor throughout the maturing process of miR-21. p-SMAD2/3 is not the only example in the literature of RNase cofactors that participate in the posttranscriptional regulation of miRNA biogenesis in both the nucleus and the cytoplasm. Transactivation-responsive DNA-binding protein-43 (TDP-43) facilitates the binding of the DROSHA complex to a subset of pri-

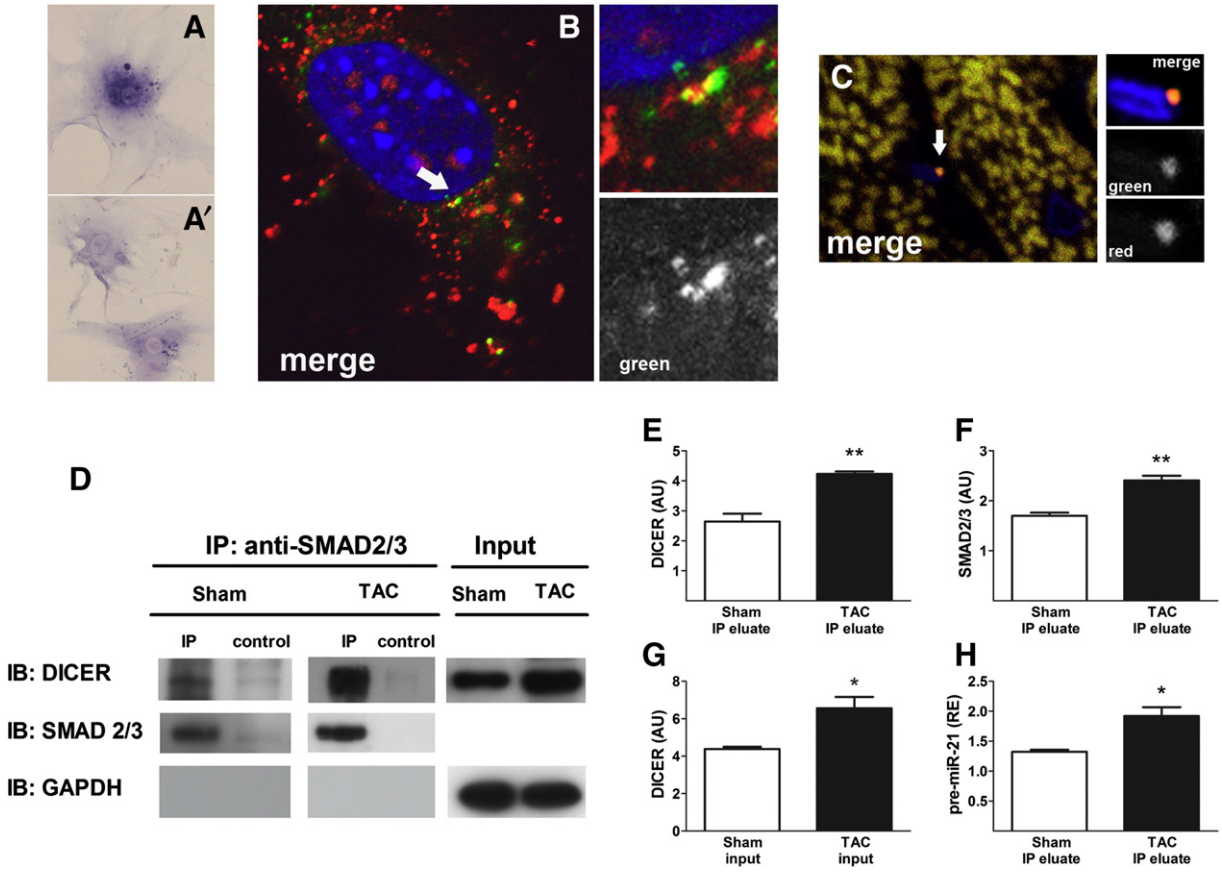

Fig. 6. SMAD2/3 forms a complex with DICER1 and pre-miR-21. A and A′: Representative in situ hybridization images showing miR-21 expression in LV primary fibroblasts cultured in the presence of TGF-β1 (0.3 ng/ml) (A) and negative control (A′). B: Representative confocal immunofluorescence images (merge channel) showing p-SMAD2/3 (red) and DICER1 (green) co-localization (yellow) in primary cardiac fibroblasts. The arrow indicates the region enlarged in the insets. DICER1 immunofluorescence (green channel) is depicted in grayscale. C: Representative LV confocal immunofluorescence images from a TAC mouse (merge channel) showing the perinuclear co-localization (yellow) of p-SMAD2/3 (red) and DICER1 (green). The cell nucleus (blue) lies in the connective tissue that wraps muscle fibers and probably belongs to a fibroblast. The arrow indicates the region of the endomysium enlarged in the insets. DICER1 (green channel) and p-SMAD2/3 (red channel) immunofluorescences are depicted in grayscale. D: LV myocardial lysates from mice sham operated or subjected to transverse aortic constriction (TAC) were immunoprecipitated with a SMAD2/3 antibody (IP) or a rabbit IgG (control). Representative images show IP and control samples immunoblotted (IB) for DICER1 and SMAD2/3. Input: representative western blot of input lysates showing DICER1 expression and GAPDH as loading control. Densitometric analyses of the immunoblots show DICER1 (E) and SMAD2/3 (F) average expressions in arbitrary units of optical density (AU). G: Densitometric analysis of the input lysates shows DICER1 average expression in AU. H: MiRNAs were extracted from the IP and subjected to qRT-PCR assay to detect co-precipitation of pre-miR-21 with DICER1 and SMAD2/3. Pre-miR-21 expression was normalized to the spike-in control cel-miR-39 and relativized to their correspondent controls (*$p < 0.05$, **$p < 0.01$ TAC vs sham, Student's *t* test).

miRNAs in the nucleus resulting in their efficient cleavage into pre-miRNAs. In the cytoplasm, TDP-43 interacts with the DICER complex to facilitate the processing of the same pre-miRNAs [37].

TGF-β1 signaling pathways are finely tuned to orchestrate the generation of cardiac fibrosis. Heart injury induces TGF-β1 overexpression that, in turn, activates miR-21 transcription and posttranscriptional maturation (present results and [23–25]). Most elements of the TGF-β signaling pathways can be targeted by one or more miRNAs and the effects of this family of cytokines are highly influenced by autoregulatory feedback loops between TGF-β and miRNAs [30]. The possibility of a direct autoregulatory process of miR-21 and TGF-β is dismissed by the negative results of TGF-β 3′UTR regulation. We suggest that TGF-β1 transcripts are not directly targeted by miR-21 while the positive control (3′UTR of SMAD7 mRNA) is inhibited in this cell line [38]. Other reported remodeling-related miR-21 targets, such as TIMP-3 whose deficiency accentuates LV hypertrophy with TAC [39], or TGF-βR2 did not exhibit any variation in TAC mice, and their expression levels did not correlate inversely with miR-21 levels, as would be expected for a miR-target.

Pressure overload of the LV is a clinical condition associated with pathological entities very prevalent in western countries, such as aortic valve stenosis or hypertension. Typically, the myocardium develops a maladaptive response to sustained hemodynamic load, which is characterized by cardiomyocyte hypertrophy and interstitial fibrosis. The development of interstitial fibrosis is a major cause of LV wall stiffening, diastolic and/or systolic dysfunction and progression to heart failure [1]. The critical role played by an excessive release of TGF-β in the LV structural damage produced by biomechanical stress is well known [17,18]. Several reports support the contribution of miR-21, as downstream effector of TGF-β, to such pathological fibrotic processes in the AS clinical scenario and in animal models [13–16]. In addition to identifying SMAD2/3 as DICER1 cofactors to the fine tuning of miR-21 expression, the present study supports that this regulatory mechanism can have pathogenetic significance in the LV remodeling associated with pressure overload in mice and humans.

The rationale of such statement is based in three major features. (i) Primary fibroblasts from mouse heart present co-localization of p-SMAD2/3 and DICER and co-immunoprecipitation–RT-qPCR assays provide direct evidence for the assembly of DICER1–SMAD2/3 complexes that co-precipitated in LV myocardial lysates from mice exposed to TAC. Moreover, the RT-q-PCR performed in the miRNAs extracted from the immunoprecipitated material evidenced the presence of pre-miR-21 associated with the DICER1 maturation complex. Compared to sham, TAC mice exhibited an enhanced association of SMAD2/3 with DICER1 and pre-miR-21. (ii) DICER1 overexpression was a response of the heart to the biomechanical stress common to the animal model

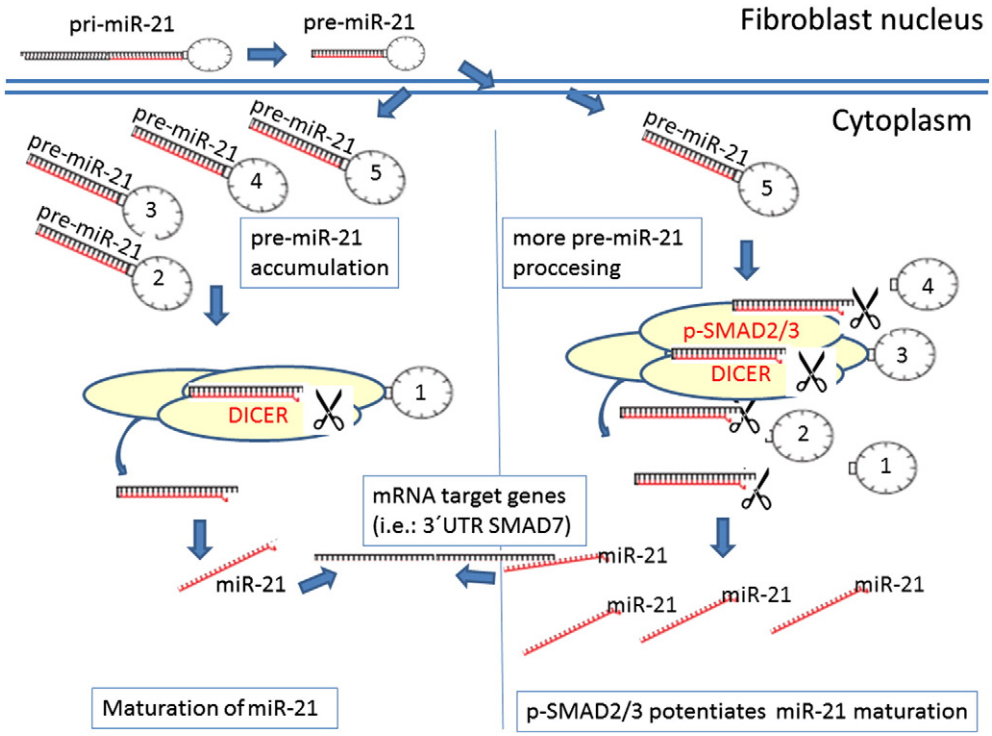

Fig. 7. Schematic representation of miR-21 processing by DICER1 in the absence or in the presence of p-SMAD2/3 in fibroblasts. The primary transcript pri-miR-21 is processed to the precursor pre-miR-21, which is translocated to the cytosol to continue its maturation. In the cytoplasm, pre-miR-21 is processed by the ribonuclease DICER1 into mature miR-21. We propose that p-SMAD2/3 potentiates posttranscriptional processing of miR-21 through a direct protein–protein interaction with DICER1 in the pre-miR-21 maturation complex. Thus, the absence of p-SMAD2/3 in the DICER1 complex would result in reduced production of mature miR-21 and accumulation of the precursor pre-miR-21. In the opposite direction, an increased presence of p-SMAD2/3 in the DICER1 maturation complex (right panel) would facilitate miR-21 production, reducing the quantity of pre-miR-21.

and human AS. The results obtained in TAC mice indicated that DICER1 up-regulation constitutes an early response to pressure overload. DICER1 overexpression was also present in the LV from 2-week-TACmice and in the LV biopsies from surgical patients suffering from severe AS, which suggests that altered biogenesis of miRNAs constitutes a persistent response to the pressure overload condition, and (iii) DICER1 expression displayed a significant positive correlation with genes encoding TGF-β1 and its major intracellular effectors, SMAD2 and SMAD3, in the LV myocardium from both TAC mice and AS patients. The relationship between DICER1 expression and TGF-β signaling molecules triggered by pressure overload in mice was further supported by the results of multiple regression analysis showing that the transcript levels of TGF-β1, SMAD2 and SMAD3 constituted independent predictors which can explain as much as 70% of the variance in DICER1 mRNA levels early after TAC.

We conclude that p-SMAD2/3 controls the posttranscriptional processing of miR-21 through a direct proteinprotein interaction between its canonical transducers p-SMAD2/3 and the ribonuclease DICER1 in the pre-miR-21 maturation complex (a schematic representation is depicted in Fig. 7). This new TGFβ-dependent facilitator mechanism could contribute to the pathogenesis of pressure overload-induced myocardial remodeling in the mouse model and in patients with aortic stenosis. In summary, our present findings contribute to a better understanding of the mechanism by which miR-21 maturation is regulated by TGF-β signaling, provide further insight into the pathophysiology of myocardial remodeling and open new avenues of research to ascertain whether the mechanism described in this manuscript operates also for other miRNAs and in other diseases.

Sources of funding

This work was supported by: Ministerio de Economía y Competitividad: Instituto de Salud Carlos III [(PI12/00999); Red de Investigación Cardiovascular (RD12/0042/0018, RD12/0042/0009)] and SAF2013-47434-Retos. National Institutes of Health R01HL107953 and R01HL106063. Foundation Leducq Transatlantic Network of Excellence.

Disclosures

None.

Transparency document

The Transparency document associated with this article can be found, in the online version.

Acknowledgments

We acknowledge the technical assistance of Amalia Cavayé (HUMV), Ana Cayón (IDIVAL), Nieves García (UC), Elena Martín (RN, HUMV), Roberto Moreta (RN, HUMV), María Navarro (IDIVAL) and Fidel Madrazo (confocal microscopy, IDIVAL).

Appendix A. Supplementary data

Supplementary data to this article can be found online at http://dx.doi.org/10.1016/j.bbadis.2015.04.006.

References

[1] J.A. Hill, E.N. Olson, Cardiac plasticity, N. Engl. J. Med. 358 (2008) 1370–1380, http://dx.doi.org/10.1056/NEJMra072139.
[2] D.P. Bartel, MicroRNAs: genomics, biogenesis, mechanism, and function, Cell 116 (2004) 281–297, http://dx.doi.org/10.1016/S0092-8674(04)00045-5.

[3] Y. Lee, C. Ahn, J. Han, H. Choi, J. Kim, J. Yim, J. Lee, P. Provost, O. Rådmark, S. Kim, V.N. Kim, The nuclear RNase III Drosha initiates microRNA processing, Nature 425 (2003) 415–419, http://dx.doi.org/10.1038/nature01957.
[4] R.I. Gregory, K.P. Yan, G. Amuthan, T. Chendrimada, B. Doratotaj, N. Cooch, R. Shiekhattar, The Microprocessor complex mediates the genesis of microRNAs, Nature 432 (2004) 235–240, http://dx.doi.org/10.1038/nature03049.
[5] S. Kawai, A. Amano, BRCA1 regulates microRNA biogenesis via the DROSHA microprocessor complex, J. Cell Biol. 197 (2012) 201–208, http://dx.doi.org/10.1083/jcb.201110008.
[6] J.E. Park, I. Heo, Y. Tian, D.K. Simanshu, H. Chang, D. Jee, D.J. Patel, V.N. Kim, Dicer recognizes the 5′ end of RNA for efficient and accurate processing, Nature 475 (2011) 201–205, http://dx.doi.org/10.1038/nature10198.
[7] K.H. Kok, M.H. Ng, Y.P. Ching, D.Y. Jin, Human TRBP and PACT directly interact with each other and associate with Dicer to facilitate the production of small interfering RNA, J. Biol. Chem. 282 (2007) 17649–17657 (doi:rna.283207[pii].10.1261/rna.283207).
[8] T.P. Chendrimada, R.I. Gregory, E. Kumaraswamy, J. Norman, N. Cooch, K. Nishikura, R. Shiekhattar, TRBP recruits the Dicer complex to Ago2 for microRNA processing and gene silencing, Nature 436 (2005) 740–744, http://dx.doi.org/10.1038/nature03868.
[9] T. Kawamata, Y. Tomari, Making RISC, Trends Biochem. Sci. 35 (2010) 368–376, http://dx.doi.org/10.1016/j.tibs.2010.03.009.
[10] E. van Rooij, A.L. Purcell, A.A. Levin, Developing microRNA therapeutics, Circ. Res. 110 (2012) 496–507, http://dx.doi.org/10.1161/CIRCRESAHA.111.247916.
[11] S. Dangwal, T. Thum, microRNA therapeutics in cardiovascular disease models, Annu. Rev. Pharmacol. Toxicol. 54 (2014) 185–203, http://dx.doi.org/10.1146/annurev-pharmtox-011613-135957.
[12] G. Condorelli, M.V. Latronico, E. Cavarretta, microRNAs in cardiovascular diseases: current knowledge and the road ahead, J. Am. Coll. Cardiol. 63 (2014) 2177–2187, http://dx.doi.org/10.1016/j.jacc.2014.01.050.
[13] T. Thum, C. Gross, J. Fiedler, T. Fischer, S. Kissler, M. Bussen, P. Galuppo, S. Just, W. Rottbauer, S. Frantz, M. Castoldi, J. Soutschek, V. Koteliansky, A. Rosenwald, M.A. Basson, J.D. Licht, J.T. Pena, S.H. Rouhanifard, M.U. Muckenthaler, T. Tuschl, G.R. Martin, J. Bauersachs, S. Engelhardt, MicroRNA-21 contributes to myocardial disease by stimulating MAP kinase signalling in fibroblasts, Nature 456 (2008) 980–984, http://dx.doi.org/10.1038/nature07511.
[14] A.J. Tijsen, Y.M. Pinto, E.E. Creemers, Non-cardiomyocyte microRNAs in heart failure, Cardiovasc. Res. 93 (2012) 573–582, http://dx.doi.org/10.1093/cvr/cvr344.
[15] A.V. Villar, R. García, M. Llano, M. Cobo, D. Merino, A. Lantero, M. Tramullas, J.M. Hurlé, M.A. Hurlé, J.F. Nistal, BAMBI (BMP and activin membrane-bound inhibitor) protects the murine heart from pressure-overload biomechanical stress by restraining TGF-β signaling, Biochim. Biophys. Acta Mol. Basis Dis. 1832 (2013) 323–335, http://dx.doi.org/10.1016/j.bbadis.2012.11.007.
[16] C. Bang, S. Batkai, S. Dangwal, S.K. Gupta, A. Foinquinos, A. Holzmann, A. Just, J. Remke, K. Zimmer, A. Zeug, E. Ponimaskin, A. Schmiedl, X. Yin, M. Mayr, R. Halder, A. Fischer, S. Engelhardt, Y. Wei, A. Schober, J. Fiedler, T. Thum, Cardiac fibroblast-derived microRNA passenger strand-enriched exosomes mediate cardiomyocyte hypertrophy, J. Clin. Invest. 124 (2014) 2136–2146, http://dx.doi.org/10.1172/JCI70577.
[17] M. Dobaczewski, W. Chen, N.G. Frangogiannis, Transforming growth factor (TGF)-β signaling in cardiac remodeling, J. Mol. Cell. Cardiol. 51 (2011) 600–606, http://dx.doi.org/10.1016/j.yjmcc.2010.10.033.
[18] E.E. Creemers, Y.M. Pinto, Molecular mechanisms that control interstitial fibrosis in the pressure-overloaded heart, Cardiovasc. Res. 89 (2011) 265–272, http://dx.doi.org/10.1093/cvr/cvq308.
[19] G. Liu, A. Friggeri, Y. Yang, J. Milosevic, Q. Ding, V.J. Thannickal, N. Kaminski, E. Abraham, miR-21 mediates fibrogenic activation of pulmonary fibroblasts and lung fibrosis, J. Exp. Med. 207 (2010) 1589–1597, http://dx.doi.org/10.1084/jem.20100035.
[20] X. Zhong, A.C. Chung, H.Y. Chen, X.M. Meng, H.Y. Lan, Smad3-mediated upregulation of miR-21 promotes renal fibrosis, J. Am. Soc. Nephrol. 22 (2011) 1668–1681, http://dx.doi.org/10.1681/ASN.2010111168.
[21] H. Zhu, H. Luo, Y. Li, Y. Zhou, Y. Zhou, Y. Jiang, J. Chai, X. Xiao, Y. You, X. Zuo, MicroRNA-21 in scleroderma fibrosis and its function in TGF-β-regulated fibrosis-related genes expression, J. Clin. Immunol. 33 (2013) 1100–1109, http://dx.doi.org/10.1007/s10875-013-9896-z.
[22] A.V. Villar, R. García, D. Merino, M. Llano, M. Cobo, C. Montalvo, R. Martín-Durán, M.A. Hurlé, J.F. Nistal, Myocardial and circulating levels of microRNA-21 reflect left ventricular fibrosis in aortic stenosis patients, Int. J. Cardiol. 167 (2013) 2875–2878, http://dx.doi.org/10.1016/j.ijcard.2012.07.021.
[23] B.N. Davis, A.C. Hilyard, G. Lagna, A. Hata, SMAD proteins control DROSHA-mediated microRNA maturation, Nature 454 (2008) 56–61, http://dx.doi.org/10.1038/nature07086.
[24] B.N. Davis, A.C. Hilyard, P.H. Nguyen, G. Lagna, A. Hata, Smad proteins bind a conserved RNA sequence to promote microRNA maturation by Drosha, Mol. Cell 39 (2010) 373–384, http://dx.doi.org/10.1016/j.molcel.2010.07.011.
[25] B.N. Davis-Dusenbery, A. Hata, Smad-mediated miRNA processing: a critical role for a conserved RNA sequence, RNA Biol. 8 (2011) 71–76, http://dx.doi.org/10.4161/rna.8.1.14299.
[26] O. Söderberg, M. Gullberg, M. Jarvius, K. Ridderstråle, K.J. Leuchowius, J. Jarvius, K. Wester, P. Hydbring, F. Bahram, L.G. Larsson, U. Landegren, Direct observation of individual endogenous protein complexes in situ by proximity ligation, Nat. Methods 3 (2006) 995–1000, http://dx.doi.org/10.1038/nmeth947.
[27] O. Söderberg, K.J. Leuchowius, M. Gullberg, M. Jarvius, I. Weibrecht, L.G. Larsson, U. Landegren, Characterizing proteins and their interactions in cells and tissues using the in situ proximity ligation assay, Methods 45 (2008) 227–232, http://dx.doi.org/10.1016/j.ymeth.2008.06.014.
[28] S. Dangwal, C. Bang, T. Thum, Novel techniques and targets in cardiovascular microRNA research, Cardiovasc. Res. 93 (2012) 545–554, http://dx.doi.org/10.1093/cvr/cvr297.
[29] S.A. Glantz, B.K. Slinker, Primer of Applied Regression and Analysis of Variance, 2nd ed. McGraw-Hill, New York, 2000.
[30] M.T. Blahna, A. Hata, Regulation of miRNA biogenesis as an integrated component of growth factor signaling, Curr. Opin. Cell Biol. 25 (2013) 233–242, http://dx.doi.org/10.1016/j.ceb.2012.12.005.
[31] L. Stalder, W. Heusermann, L. Sokol, D. Trojer, J. Wirz, J. Hean, A. Fritzsche, F. Aeschimann, V. Pfanzagl, P. Basselet, J. Weiler, M. Hintersteiner, D.V. Morrissey, N.C. Meisner-Kober, The rough endoplasmatic reticulum is a central nucleation site of siRNA-mediated RNA silencing, EMBO J. 32 (2013) 1115–1127, http://dx.doi.org/10.1038/emboj.2013.52.
[32] P. Hoffer, S. Ivashuta, O. Pontes, A. Vitins, C. Pikaard, A. Mroczka, N. Wagner, T. Voelker, Posttranscriptional gene silencing in nuclei, Proc. Natl. Acad. Sci. U. S. A. 108 (2011) 409–414, http://dx.doi.org/10.1073/pnas.1009805108.
[33] A.D. Redfern, S.M. Colley, D.J. Beveridge, N. Ikeda, M.R. Epis, X. Li, C.E. Foulds, L.M. Stuart, A. Barker, V.J. Russell, K. Ramsay, S.J. Kobelke, X. Li, E.C. Hatchell, C. Payne, K.M. Giles, A. Messineo, A. Gatignol, R.B. Lanz, B.W. O'Malley, P.J. Leedman, RNA-induced silencing complex (RISC) proteins PACT, TRBP, and Dicer are SRA binding nuclear receptor coregulators, Proc. Natl. Acad. Sci. U. S. A. 110 (2013) 6536–6541, http://dx.doi.org/10.1073/pnas.1301620110.
[34] M.A. Newman, S.M. Hammond, Emerging paradigms of regulated microRNA processing, Genes Dev. 24 (2010) 1086–1092, http://dx.doi.org/10.1101/gad.1919710.
[35] H. Siomi, M.C. Siomi, Posttranscriptional regulation of microRNA biogenesis in animals, Mol. Cell 38 (2010) 323–332, http://dx.doi.org/10.1016/j.molcel.2010.03.013.
[36] J. Krol, I. Loedige, W. Filipowicz, The widespread regulation of microRNA biogenesis, function and decay, Nat. Rev. Genet. 11 (2010) 597–610, http://dx.doi.org/10.1038/nrg2843.
[37] Y. Kawahara, A. Mieda-Sato, TDP-43 promotes microRNA biogenesis as a component of the Drosha and Dicer complexes, Proc. Natl. Acad. Sci. U. S. A. 109 (2012) 3347–3352, http://dx.doi.org/10.1073/pnas.1112427109.
[38] L.H. Wei, X.R. Huang, Y. Zhang, Y.Q. Li, H.Y. Chen, R. Heuchel, B.P. Yan, C.M. Yu, H.Y. Lan, Deficiency of Smad7 enhances cardiac remodeling induced by angiotensin II infusion in a mouse model of hypertension, PLoS One 8 (2013) e70195, http://dx.doi.org/10.1371/journal.pone.0070195.
[39] Z. Kassiri, G.Y. Oudit, O. Sanchez, F. Dawood, F.F. Mohammed, R.K. Nuttall, D.R. Edwards, P.P. Liu, P.H. Backx, R. Khokha, Combination of tumor necrosis factor-alpha ablation and matrix metalloproteinase inhibition prevents heart failure after pressure overload in tissue inhibitor of metalloproteinase-3 knock-out mice, Circ. Res. 19 (2005) 380–390, http://dx.doi.org/10.1161/01.RES.0000178789.16929.cf.